

Crystal Structure and Electronic States of Co and Gd Ions in a $\text{Gd}_{0.4}\text{Sr}_{0.6}\text{CoO}_{2.85}$ Single Crystal

M. S. Platonov^{a*}, V. A. Dudnikov^a, Yu. S. Orlov^a, N. V. Kazak^a, L. A. Solovyov^b,
Ya. V. Zubavichus^c, A. A. Veligzhanin^c, P. V. Dorovatovskii^c, S. N. Vereshchagin^b,
K. A. Shaykhutdinov^a, and S. G. Ovchinnikov^{a, d}

^a Kirensky Institute of Physics, Siberian Branch, Russian Academy of Sciences,
Akademgorodok, Krasnoyarsk, 660036 Russia

^b Institute of Chemistry and Chemical Technology, Siberian Branch, Russian Academy of Sciences,
Krasnoyarsk, 660036 Russia

^c National Research Centre Kurchatov Institute, pl. Akademika Kurchatova 1, Moscow, 123182 Russia

^d National Research Nuclear University MEPhI, Kashirskoe sh. 31, Moscow, 115409 Russia

*e-mail: platonov@iph.krasn.ru

Received December 9, 2015; in final form, December 18, 2015

X-ray diffraction and X-ray absorption near edge structure (XANES) spectra have been measured at the Co K -edge and Gd L_3 -edge in GdCoO_3 and $\text{Gd}_{0.4}\text{Sr}_{0.6}\text{CoO}_{2.85}$ cobaltites. The effect of Sr substitution on the crystal structure and electronic and magnetic states of Co^{3+} ions in a $\text{Gd}_{0.4}\text{Sr}_{0.6}\text{CoO}_{2.85}$ single crystal has been analyzed. The XANES measurements at the Co K -edge have not showed a noticeable shift of the absorption edge with an increase in the concentration of Sr. This indicates that the effective valence of cobalt does not change. An increase in the intensity of absorption at the Gd L_3 -edge is due to an increase in the degree of hybridization of the Gd($5d$) and O($2p$) states. The effect of hole doping on the magnetic properties results in the appearance of the ferromagnetic component and in a significant increase in the magnetic moment.

DOI: 10.1134/S0021364016030139

1. INTRODUCTION

Rare-earth cobaltites RCoO_3 (where R is a rare-earth ion) doped with bivalent alkaline ions constitute a class of materials with unique physical properties [1]. These compounds in the undoped state, as well as high-temperature superconducting cuprates and manganites RMnO_3 , are Mott insulators. As in manganites, hole doping leads to the appearance of conduction and a magnetic order. The cobaltites have a specificity caused by competition between various spin states of the Co^{3+} ion. For unsubstituted cobaltites RCoO_3 , among which LaCoO_3 is most studied, it was established that the ground state is formed by a non-magnetic low-spin state LS ($S=0$), whereas high-spin states HS ($S=2$) become occupied with an increase in the temperature [2, 3]. Our detailed study [4] of GdCoO_3 also showed that Co^{3+} at low temperatures is in the LS state and the HS states form the temperature-dependent effective moment.

In this work, we study the $\text{Gd}_{0.4}\text{Sr}_{0.6}\text{CoO}_{2.85}$ single crystal as an example of substituted cobaltites. The simplest hypothesis of the appearance of Co^{4+} ions at hole doping with a nonzero magnetic moment seemingly corresponds to the revealed magnetic state at low

temperatures. However, the analysis of XANES spectra at Co- and Gd-ion edges does not confirm this hypothesis and indicates a more complex nature of hole states at the top of the valence band formed by the hybridization of the O(p), Co($3d$), and Gd($5d$) states.

2. SAMPLES AND EXPERIMENTAL TECHNIQUES

The $\text{Gd}_{0.4}\text{Sr}_{0.6}\text{CoO}_{3-\delta}$ single crystal was obtained by the optical floating zone method. To synthesize the initial charge, the stoichiometric amounts of oxides Co_3O_4 (99.7%), Gd_2O_3 (99.99%), and SrCO_3 (99.99%) were carefully mixed in ethanol in a jasper mortar. After drying, the mixture thus obtained was annealed at a temperature of 1200°C in a platinum crucible for 24 h in air with multiple repetition of milling–annealing cycles. Further, cylindrical rods with a diameter of 6 mm and a length of 80 mm were pressed from the synthesized powder by hydrostatic compression. The rods were sintered in air at a temperature of 1650°C for 10 h, were then placed in an FZ-T-4000-H optical floating zone furnace, and were heating to melting. The growth rate was 2 mm/h and the rate of relative rotation of rods was 30 rpm. Argon at normal

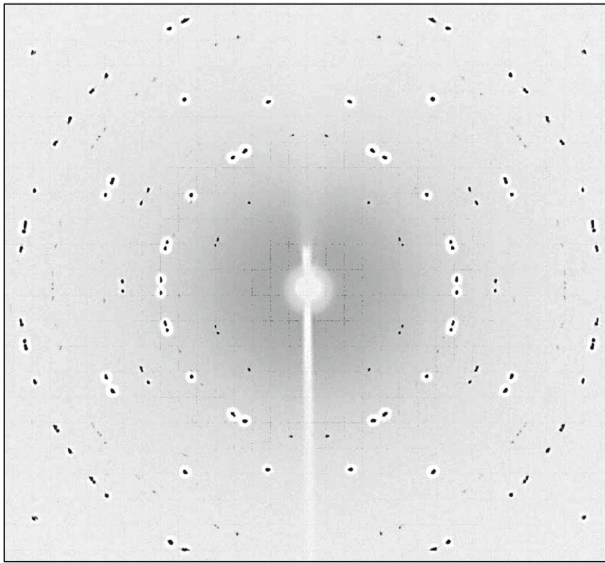


Fig. 1. Result of the φ -scanning of the $\text{Gd}_{0.4}\text{Sr}_{0.6}\text{CoO}_{2.85}$ sample demonstrating the characteristic diffraction pattern from a single crystal. The scanning covers the total angular range of 360° about the vertical axis.

pressure was used as a gaseous medium. The resulting remelted rod had a diameter of ~ 5 mm and a length of ~ 70 mm. The central part of the rod was studied. The technology of producing polycrystalline GdCoO_3 was described in detail in [4], where X-ray diffraction data were also reported.

The crystal structure was analyzed in $\text{Cu } K_\alpha$ radiation on a PANalytical X'Pert Pro powder diffractometer at room temperature. The angular range $2\Theta = 10^\circ - 90^\circ$ was scanned with a step of 0.013° . The lattice parameters were determined from the positions of diffraction maxima with the use of the ITO code [5]. The refinement of the crystal structure was performed from the total profile of the diffraction patterns with the Rietveld method [6] and the minimization of the derivative of the difference [7].

The single-crystal diffraction of $\text{Gd}_{0.4}\text{Sr}_{0.6}\text{CoO}_{3-\delta}$ was measured at the Belok station (K4.4e), National Research Centre Kurchatov Institute. The total angular range of 360° about the vertical axis was scanned with a step of 2° on a Rayonix SX165 matrix CCD detector at $\lambda = 0.9886 \text{ \AA}$. Figure 1 shows the result of the φ -scanning of the sample demonstrating the diffraction pattern characteristic of a single crystal. Reliable refinement of the crystal structure was impossible

because a fraction of intensities of diffraction peaks were beyond the dynamic range of the detector.

The content of oxygen and nonstoichiometry index δ were determined from the loss of mass ($\Delta m, \%$), which was measured at the thermogravimetric reconstruction, under the assumption that cobalt is reduced to a metallic state [8]. The reduction was performed with an NETZSCH STA 449C analyzer equipped with an AeolosQMS 403C mass spectrometer. The experiment was carried out in an argon flow with 5% H_2 at the heating of the sample to 900°C with a rate of 10° per minute. For crystalline $\text{Gd}_{0.4}\text{Sr}_{0.6}\text{CoO}_{3-\delta}$, we obtained $\delta = 0.15 \pm 0.01$. Below, we use the formula $\text{Gd}_{0.4}\text{Sr}_{0.6}\text{CoO}_{2.85}$.

The XANES and extended X-ray absorption fine structure (EXAFS) spectra at the Co K -edge and Gd L_3 -edge in GdCoO_3 and $\text{Gd}_{0.4}\text{Sr}_{0.6}\text{CoO}_{2.85}$ were measured at the STM station (K1.3b), National Research Centre Kurchatov Institute. The absorption spectra were recorded in the transmission geometry at room temperature. A channel-cut Si(111) single crystal monochromator was used providing an energy resolution of $\Delta E/E \sim 2 \times 10^{-4}$. The scanning step in the XANES range was ~ 0.4 eV. The signal accumulation time was 4 s per point. The samples were preliminarily milled into a powder, which was then deposited on a thin kapton film with a gluing layer in order to ensure uniform absorption.

The field and temperature dependences of the magnetization were measured on a vibration magnetometer [9] in magnetic fields to 60 kOe. The relative error of measurements is no more than the width of lines shown in the figures.

3. EXPERIMENTAL RESULTS AND DISCUSSION

3.1. X-ray Diffraction

Figure 2 shows the diffraction pattern of $\text{Gd}_{0.4}\text{Sr}_{0.6}\text{CoO}_{2.85}$. The analysis of the positions of reflections and systematic extinctions revealed a rhombic crystal system (space group $Imam$). The lattice parameters are summarized in Table 1 in comparison with the data for GdCoO_3 . Atoms of Gd and Sr equiprobably occupy site A in $\text{Gd}_{0.4}\text{Sr}_{0.6}\text{CoO}_3$. There are two nonequivalent oxygen sites. Anion vacancies are distributed randomly. The replacement of Gd^{3+} ions (ion radius $r_{\text{Gd}^{3+}} = 1.215 \text{ \AA}$) by Sr^{2+} ions with a larger ion radius $r_{\text{Sr}^{2+}} = 1.44 \text{ \AA}$ [10] results in an

Table 1. Lattice parameters of cobaltites

	Space group	$a, \text{ \AA}$	$b, \text{ \AA}$	$c, \text{ \AA}$	$V, \text{ \AA}^3$
GdCoO_3	$Pbnm$	5.22591(4)	5.39095(5)	7.45565(6)	210.045(3)
$\text{Gd}_{0.4}\text{Sr}_{0.6}\text{CoO}_{2.85}$	$Imam$	5.3601(6)	5.3785(7)	7.5751(11)	218.38(5)

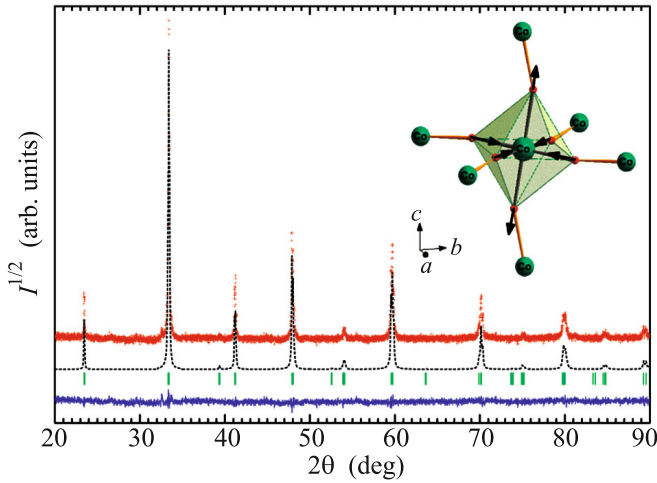


Fig. 2. (Color online) (Red line) Experimental, (black dotted line) calculated, and (blue line) difference X-ray diffraction patterns of $\text{Gd}_{0.4}\text{Sr}_{0.6}\text{CoO}_{2.85}$ obtained by the full-profile refinement of the crystal structure. The calculated positions of the reflections are shown by dashes. The inset shows the local distortions of the CoO_6 coordination octahedron in $\text{Gd}_{0.4}\text{Sr}_{0.6}\text{CoO}_{2.85}$. Arrows indicate compression and extension.

increase in the lattice parameters a and c . The volume of the unit cell increases by $\sim 4\%$. The average interatomic distances and angles of the Co–O–Co bonds are presented in Table 2. It is seen that the distances $\langle \text{Gd}/\text{Sr}-\text{O} \rangle$ vary only slightly with an increase in the content of Sr. In this case, the nearest environment of Gd atoms becomes more regular. The main effect of substitution is an increase in local distortions of the coordination octahedron CoO_6 and in the angles of the Co–O–Co bonds. The distribution of the interionic distances in GdCoO_3 is such that the oxygen octahedron around the Co^{3+} ion is compressed (four long distances, 1.936 and 1.942 Å, lie in the ab plane, whereas two short distances, 1.919 Å, are parallel to the c axis). The addition of Sr results in a significant elongation of the Co–O bond along the c axis (two long distances are ~ 1.925 Å), which is accompanied by a strong compression of the ab plane (four short distances are ~ 1.904 Å). As a result, the average interatomic distance $\langle \text{Co}-\text{O} \rangle$ decreases significantly: 1.932 Å for GdCoO_3 and 1.911 Å for $\text{Gd}_{0.4}\text{Sr}_{0.6}\text{CoO}_{2.85}$ (inset in Fig. 2). Changes in the second coordination sphere of cobalt atoms are due to an increase in the

Table 2. Average interatomic distances and angles of bonds in cobaltites

	$\langle \text{Gd}/\text{Sr}-\text{O} \rangle$, Å	$\langle \text{Co}-\text{O} \rangle$, Å	$\langle \text{Co}-\text{O}-\text{Co} \rangle$, deg
GdCoO_3	2.686(2)	1.932(2)	151.4(2)
$\text{Gd}_{0.4}\text{Sr}_{0.6}\text{CoO}_{2.85}$	2.688(18)	1.911(4)	167(2)

angles of the Co–O–Co bonds, particularly in the ab plane (150.9° for GdCoO_3 and 170.9° for $\text{Gd}_{0.4}\text{Sr}_{0.6}\text{CoO}_{2.85}$). Thus, the introduction of Sr leads to an increase in low-symmetry tetragonal Jahn–Teller distortions (Q_3).

3.2. XANES Spectroscopy

The chemical formula, namely, the relation between the numbers of Gd and Co atoms, was more precisely determined from a jump of the absorption edge using the expression

$$\frac{N_{\text{Gd}}}{N_{\text{Co}}} = \frac{\Delta(\mu t)_{\text{Gd}} 1/\Delta(\mu/\rho)_{\text{Gd}} 1/M_{\text{Gd}}}{\Delta(\mu t)_{\text{Co}} 1/\Delta(\mu/\rho)_{\text{Co}} 1/M_{\text{Co}}}, \quad (1)$$

where N_{Gd} and N_{Co} are the numbers of Gd and Co atoms in the sample, respectively; $\Delta(\mu t)$ is the absorption jump; M is the molecular mass; and $\Delta(\mu/\rho)$ is the jump of the mass absorption coefficient. The error was no more than 5%. With the ratio $N_{\text{Gd}}/N_{\text{Co}} = 0.38/1$ thus determined, the chemical formula of the single crystal is $\text{Gd}_{0.4}\text{Sr}_{0.6}\text{CoO}_{2.85}$.

Figure 3 shows the normalized XANES spectra of GdCoO_3 and $\text{Gd}_{0.4}\text{Sr}_{0.6}\text{CoO}_{2.85}$ measured at the Co K -edge and Gd L_3 -edge at room temperature. Metallic Co and CoO (Co^{2+}) and Co_2O_3 (Co^{3+}) oxides were used as references for the determination of Co ion charge. The positions of the absorption edges of the references are presented on the upper scale in Fig. 3. The absorption maximum (at ~ 7727 eV) corresponds to the $1s-4p$ dipole transition [11]. The Sr substitution does not result in any noticeable shift of the Co absorption edge. The energy position of the edge ($E_0 = 7724$ eV), which was determined from the maximum of the first derivative, is close for both samples to the corresponding value in Co_2O_3 (Co^{3+}). The found value E_0 is in agreement with the data previously reported for unsubstituted cobaltites LaCoO_3 and EuCoO_3 [11–13].

The effect of Sr substitution on the local electronic structure of Gd was studied by measuring the XANES spectra at the Gd L_3 -edge. Figure 4 shows the XANES spectra of GdCoO_3 and $\text{Gd}_{0.4}\text{Sr}_{0.6}\text{CoO}_{2.85}$, as well as of Gd_2O_3 as the Gd^{3+} reference. The maximum at ~ 7248 eV is due to the $2p_{3/2}-5d$ dipole transition in the Gd^{3+} ($4f^7$) ion. The intensity of the white line increases with the content of Sr. According to the X-ray diffraction analysis, the interionic distances $\langle \text{Gd}/\text{Sr}-\text{O} \rangle$ hardly change at substitution (2.686 Å in GdCoO_3 and 2.688 Å in $\text{Gd}_{0.4}\text{Sr}_{0.6}\text{CoO}_{2.85}$). At the same time, the nearest environment of the Gd atom becomes more regular and can change the degree of hybridization of Gd($5d$) and O($2p$) states [14].

Thus, the XANES measurements showed that, with an increase in the content of Sr^{2+} , first, the Co K absorption edge is not shifted, which can indicate that the effective valence of Co (Co^{3+}) does not change,

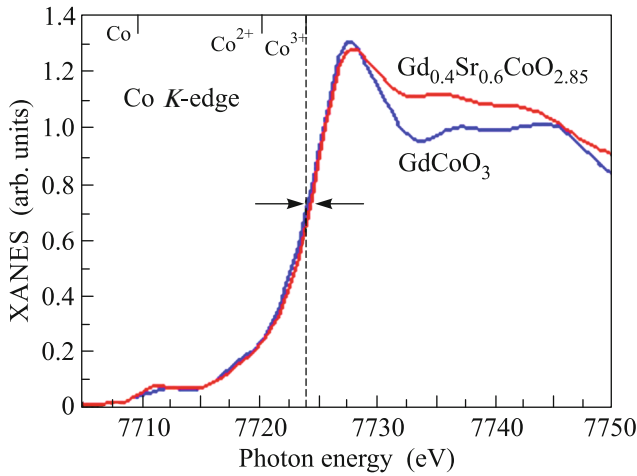


Fig. 3. (Color online) XANES spectra at the Co K -edge for the compounds $\text{Gd}_{1-x}\text{Sr}_x\text{CoO}_{3-\delta}$ ($x = 0.0, 0.6$). The dashed vertical straight line marks the energy of the absorption edge of the samples.

and, second, the intensity of the $2p-5d$ dipole transition in the Gd ion increases.

3.3. Magnetization

Figure 5 shows the field dependences of the magnetization of GdCoO_3 and $\text{Gd}_{0.4}\text{Sr}_{0.6}\text{CoO}_{2.85}$ measured at liquid helium temperatures. The magnetization of $\text{Gd}_{0.4}\text{Sr}_{0.6}\text{CoO}_{2.85}$ is the superposition of two contributions: parametric from Gd^{3+} ions and ferromagnetic associated with the Co–O magnetic subsystem. Owing to the paramagnetic contribution from Gd^{3+} ions, magnetic saturation does not occur in fields up to 60 kOe. The ferromagnetic contribution is manifested in the form of a hysteresis loop with the

coercive force $H_c = 1.1$ kOe. The remanent magnetization in GdCoO_3 ($\sim 6 \mu_B/\text{f.u.}$) is close to $7 \mu_B/\text{f.u.}$ expected for the $^8S_{7/2}$ ground state of the Gd^{3+} ion. The paramagnetic contribution of Gd^{3+} ions in the $\text{Gd}_{0.4}\text{Sr}_{0.6}\text{CoO}_{2.85}$ substituted sample should give a much smaller remanent magnetization than the experimentally observed value. We estimated the magnetic moment associated with the Co–O subsystem as $\sim 1.95 \mu_B/\text{f.u.}$ The temperature of the magnetic transition in the $\text{Gd}_{0.4}\text{Sr}_{0.6}\text{CoO}_{2.85}$ substituted sample is 135 K.

4. DISCUSSION

The substitution of Sr^{2+} ions for some R-rare-earth ions should initiate the appearance of holes, which can both be localized and become charge carriers. In the case of the first scenario of hole doping, the properties of the $\text{R}_{1-x}\text{Sr}_x\text{CoO}_{3-\delta}$ system are considered within the concept of mixing of Co^{3+} and Co^{4+} states. The fraction of Co^{4+} increases monotonically with the concentration x [15, 16]. To determine the valence state of cobalt ions by XANES spectroscopy (at the Co K -edge), both the shift of the absorption edge and the shift of the main absorption maximum are used. In the case of the linear dependence between the chemical shift and the valence state of Co, an increase in the valence should lead to a visible shift of the absorption edge toward higher energies. In particular, the shift at the Co K -edge under change of Co^{2+} to Co^{3+} is about 3 eV (the upper panel in Fig. 3). The XANES studies of manganites show that the shift of the Mn K absorption edge is $\Delta E_0 = 3\text{eV}$, which is associated with change in the valence from Mn^{3+} to Mn^{4+} in LaMnO_3 and CaMnO_3 [17]. At the same time, similar studies in $\text{La}_{1-x}\text{Sr}_x\text{CoO}_3$ cobaltites indicate a weak (or absent)

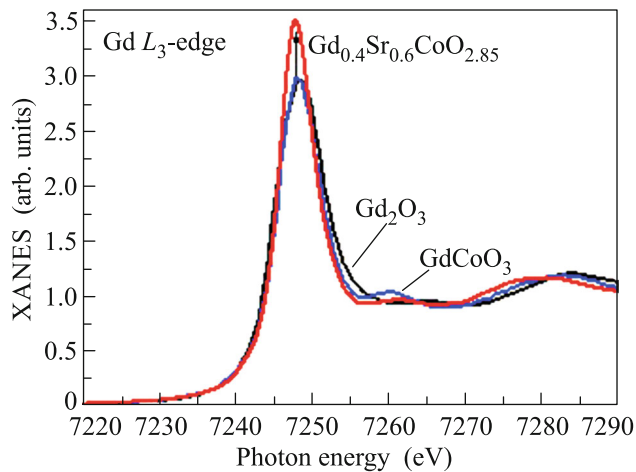


Fig. 4. (Color online) XANES spectra at the Gd L_3 edge of the compounds $\text{Gd}_{1-x}\text{Sr}_x\text{CoO}_{3-\delta}$ ($x = 0.0, 0.6$) as compared to the Gd_2O_3 reference.

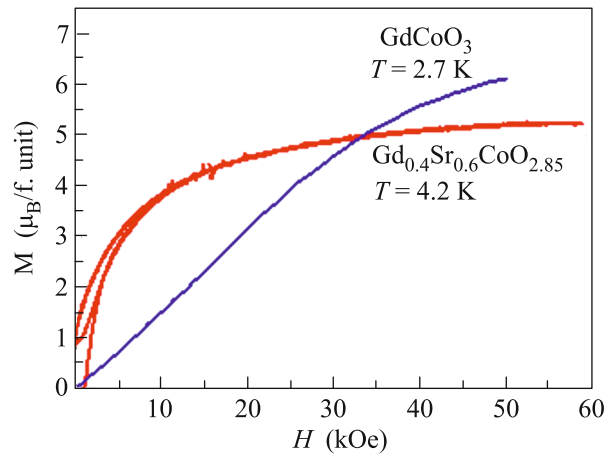


Fig. 5. (Color online) Field dependences of the magnetization of GdCoO_3 and $\text{Gd}_{0.4}\text{Sr}_{0.6}\text{CoO}_{2.85}$.

concentration dependence of the Co *K* absorption edge [18, 19].

The addition of 60% Sr to the $\text{Gd}_{0.4}\text{Sr}_{0.6}\text{CoO}_{2.85}$ sample under study in this scenario would increase in the effective valence of cobalt to $\text{Co}^{3.3+}$ (instead of Co^{3+} in GdCoO_3). Nevertheless, the experimentally detected shift of the absorption edge in $\text{Gd}_{0.4}\text{Sr}_{0.6}\text{CoO}_{2.85}$ does not exceed 0.3 eV. Consequently, we can conclude that the valence state of cobalt in substituted $\text{Gd}_{0.4}\text{Sr}_{0.6}\text{CoO}_{2.85}$ is close to Co^{3+} . The other hole doping scenario in the $\text{Gd}_{0.4}\text{Sr}_{0.6}\text{CoO}_{2.85}$ system implies that holes are partially localized on O(*2p*) states and become charge carriers (bond character). In this case, Co(*3d*) states and, therefore, the effective valence of cobalt should hardly change. The structural distortions associated with the substitution of Sr^{2+} ions for Gd^{3+} ions (changes in the interionic distances $\langle\text{Gd}/\text{Sr}-\text{O}\rangle$, $\langle\text{Co}-\text{O}\rangle$, and angles of the Co–O–Co bonds) change the degree of hybridization of Co(*3d*)–O(*2p*) and Gd(*5d*)–O(*2p*) states and increase the intensities of dipole transitions.

Holes localized in O(*2p*) states can have a magnetic moment. The interaction of unpaired spins of oxygen with the cobalt subsystem can make an additional contribution to magnetism. The XANES and X-ray magnetic circular dichroism (XMCD) measurements at the O *K*-edge experimentally confirm the appearance of holes on oxygen in the $\text{La}_{1-x}\text{Sr}_x\text{CoO}_{3\pm\delta}$ system. It was shown that an increase in *x* is accompanied by a significant increase in the intensity of absorption and a shift of the *K*-edge toward lower energies (527–529 eV), which is due to an increase in the number of unoccupied O(*2p*) states [20]. The intensity of the XMCD signal increases simultaneously, indicating a nonzero orbital angular momentum on oxygen (appearance of magnetic holes). The magnetic moment on O is parallel to the magnetic moment of Co.

To conclude, it is worth noting that the introduction of strontium in GdCoO_3 affects the crystal structure, changing the symmetry of the lattice and creating local distortions of the nearest environment of Co and Gd ions. At the same time, the electronic state of Co ions hardly changes. The appearing hybridization of O(*2p*) states with Co(*3d*) states and Gd(*5d*) states increases the intensity of dipole transitions. The introduction of strontium induces the appearance of a ferromagnetic order and increases the magnetic moment. The nature of hole states requires additional studies, including X-ray absorption spectroscopy and XMCD studies at the O *K*-edge.

This work was supported in part by the Russian Foundation for Basic Research (project nos. 13-02-00958, 13-02-00358, 14-02-31051, and 16-32-60049), by the Council of the President of the Russian Federation for Support of Young Scientists and Leading Sci-

entific Schools (project no. SP-938.2015.5), and by the program “UMNIK.” The X-ray diffraction and thermochemical studies were supported by the Siberian Branch, Russian Academy of Sciences (project no. V.45.3.1).

REFERENCES

1. N. B. Ivanova, S. G. Ovchinnikov, M. M. Korshunov, I. M. Eremin, and N. V. Kazak, *Phys. Usp.* **52**, 789 (2009).
2. M. W. Haverkort, Z. Hu, J. C. Cezar, T. Burnus, H. Hartmann, M. Reuther, C. Zobel, T. Lorenz, A. Tanaka, N. B. Brookes, H. H. Hsieh, H.-J. Lin, C. T. Chen, and L. H. Tjeng, *Phys. Rev. Lett.* **97**, 176405 (2006).
3. S. Noguchi, S. Kawamata, K. Okuda, H. Nojiri, and M. Motokawa, *Phys. Rev. B* **66**, 094404 (2002).
4. Y. S. Orlov, L. A. Solovyov, V. A. Dudnikov, A. S. Fedorov, A. A. Kuzubov, N. V. Kazak, and S. G. Ovchinnikov, *Phys. Rev. B* **88**, 235105 (2013).
5. J. W. Visser, *J. Appl. Crystallogr.* **2**, 89 (1969).
6. H. Rietveld, *J. Appl. Crystallogr.* **2**, 65 (1969).
7. L. A. Solovyov, *J. Appl. Cryst.* **37**, 743 (2004).
8. K. Conder, E. Pomjakushina, A. Soldatov, and E. Mitterberg, *Mater. Res. Bull.* **40**, 257 (2005).
9. A. D. Balaev, Yu. V. Boyarshinov, M. M. Karpenko, and B. P. Khrustalev, *Prib. Tekh. Eksp.*, No. 3, 167 (1985).
10. R. T. Shannon, *Acta Crystallogr. A* **32**, 751 (1976).
11. O. Haas, R. P. W. J. Struis, and J. M. McBreen, *J. Solid State Chem.* **177**, 1000 (2004).
12. J. Y. Chang, B. N. Lin, Y. Y. Hsu, and H. C. Ku, *Phys. B: Condens. Matter* **329**, 826 (2003).
13. F. J. Berry, J. F. Marco, and X. Ren, *J. Solid State Chem.* **178**, 961 (2005).
14. L. Chen, X. Chen, F. Liu, H. Chen, H. Wang, E. Zhao, and S. Chen, *Sci. Rep.* **5**, 11514 (2015).
15. R. P. Haggerty and R. Seshadri, *J. Phys.: Condens. Matter* **16**, 6477 (2004).
16. I. O. Troyanchuk, A. N. Chobot, N. V. Tereshko, D. V. Karpinskii, V. Efimov, V. Sikolenko, and P. Henry, *J. Exp. Theor. Phys.* **112**, 837 (2011).
17. F. Bridges, C. H. Booth, M. Anderson, G. H. Kwei, J. J. Neumeier, J. Snyder, and E. Brosha, *Phys. Rev. B* **63**, 214405 (2001).
18. O. Haas, C. Ludwig, U. Bergmann, R. N. Singh, A. Braun, and T. Graule, *J. Solid State Chem.* **184**, 3163 (2011).
19. Y. Jiang, F. Bridges, N. Sundaram, D. P. Belanger, I. E. Anderson, J. F. Mitchell, and H. Zheng, *Phys. Rev. B* **80**, 144423 (2009).
20. S. Medling, Y. Lee, H. Zheng, J. F. Mitchell, J. W. Freeland, B. N. Harmon, and F. Bridges, *Phys. Rev. Lett.* **109**, 157204 (2012).

Translated by R. Tyapae